



1 **Online measurements of cycloalkanes based on NO⁺ chemical**
2 **ionization in proton transfer reaction time of flight mass**
3 **spectrometry (PTR-ToF-MS)**

4 Yubin Chen^{1,2}, Bin Yuan^{1,2,*}, Chaomin Wang³, Sihang Wang^{1,2}, Xianjun He^{1,2},
5 Caihong Wu^{1,2}, Xin Song^{1,2}, Yibo Huangfu^{1,2}, Xiao-Bing Li^{1,2}, Yijia Liao^{1,2}, Min
6 Shao^{1,2}

7 ¹ Institute for Environmental and Climate Research, Jinan University, Guangzhou
8 511443, China

9 ² Guangdong-Hongkong-Macau Joint Laboratory of Collaborative Innovation for
10 Environmental Quality, Guangzhou 511443, China

11 ³ School of Tourism and Culture, Guangdong Eco-engineering Polytechnic,
12 Guangzhou 510520, China

13
14 *Correspondence to: Bin Yuan (byuan@jnu.edu.cn)



15 **Abstract:**

16 Cycloalkanes are important trace hydrocarbons existing in the atmosphere, and
17 they are considered as a major class of intermediate volatile organic compounds
18 (IVOCs). Laboratory experiments showed that the yields of secondary organic aerosols
19 (SOA) from oxidation of cycloalkanes are relatively higher than acyclic alkanes with
20 the same carbon number. However, measurements of cycloalkanes in the atmosphere
21 are still challenging at present. In this study, we show that online measurements of
22 cycloalkanes can be achieved using proton transfer reaction time-of-flight mass
23 spectrometry with NO^+ chemical ionization (NO^+ PTR-ToF-MS). Cyclic and bicyclic
24 alkanes are ionized with NO^+ via hydride ion transfer leading to major product ions of
25 $\text{C}_n\text{H}_{2n-1}^+$ and $\text{C}_n\text{H}_{2n-3}^+$, respectively. As isomers of cycloalkanes, alkenes undergoes
26 association reactions with major product ions of $\text{C}_n\text{H}_{2n}\cdot(\text{NO})^+$, and concentrations of
27 1-alkenes and trans-2-alkenes in the atmosphere are usually significantly lower than
28 cycloalkanes (about 25% and <5%, respectively), as the result inducing little
29 interference to cycloalkanes detection in the atmosphere. Calibration of various
30 cycloalkanes show similar sensitivities, associated with small humidity dependence.
31 Applying this method, cycloalkanes were successfully measured at an urban site in
32 southern China and a chassis dynamometer study for vehicular emissions.
33 Concentrations of both cyclic and bicyclic alkanes are significant in urban air and
34 vehicular emissions, with comparable cyclic alkanes/acyclic alkanes ratios between
35 urban air and gasoline vehicles. These results demonstrates that NO^+ PTR-ToF-MS
36 provides a new complementary approach for fast characterization of cycloalkanes in
37 both ambient air and emission sources, which can be helpful to fill the gap in
38 understanding importance of cycloalkanes in the atmosphere.

39
40



41 **1 Introduction**

42 Organic compounds, as important trace components in the atmosphere, are
43 released to the atmosphere from many different natural and anthropogenic sources,
44 which have complicated and diverse chemical compositions (de Gouw, 2005; Goldstein
45 and Galbally, 2007; He et al., 2022). Components and concentration levels of organic
46 compounds affect largely on atmospheric chemistry, atmospheric oxidation capacity,
47 and radiation balance (Monks et al., 2015; Wu et al., 2020), as well as human health
48 (Xing et al., 2018). According effective saturation concentrations (Donahue et al., 2012),
49 organic compounds can be divided into intermediate volatile organic compounds
50 (IVOCs), semi-volatile organic compounds (SVOCs), low volatile organic compounds
51 (LVOCs), and extremely low volatile organic compounds (ELVOCs). Due to high
52 yields of secondary organic aerosol (SOA) (Lim and Ziemann, 2009; Robinson et al.,
53 2007), IVOCs have been proved to be important SOA precursors in urban atmospheres
54 (Tkacik et al., 2012; Zhao et al., 2014).

55 Many studies showed that higher alkanes (i.e., linear and branched alkanes with
56 12-20 carbon atoms) to be important chemical components of IVOCs (Li et al., 2019;
57 Zhao et al., 2014). Similar to these acyclic alkanes, cycloalkanes can also account for
58 significant fractions of IVOCs. Cycloalkanes can reach more than 20% of IVOCs
59 concentrations in diesel vehicle exhausts, lubricating oil, and diesel fuels (Alam et al.,
60 2018; Liang et al., 2018; Lou et al., 2019), which are comparable or even higher than
61 linear and branched alkanes. In some oil and gas regions, high concentrations of
62 cycloalkanes were also reported (Aklilu et al., 2018; Gilman et al., 2013; Warneke et
63 al., 2014). More importantly, laboratory studies suggest that SOA yields of cyclic and
64 polycyclic alkanes are significantly higher than linear or branched alkanes with the
65 same carbon number (as high as a factor of 5) (Hunter et al., 2014; Jahn et al., 2021; Li
66 et al., 2021; Loza et al., 2014; Yee et al., 2013). As the result, cyclic and bicyclic species
67 are shown to be large contributors to SOA formation potential from vehicles (Xu et al.,
68 2020a, b; Zhao et al., 2015; Zhao et al., 2016). Recently, Hu et al. (2022) proposed that



69 IVOCs contributions to SOA formation in an urban region can increase from 8-20%
70 (acyclic alkanes only) to 17.5-46% if cycloalkanes are considered, signifying the
71 importance of cycloalkanes in SOA formation.

72 Cycloalkanes are mainly measured using gas chromatography-mass
73 spectrometer/flame ionization detector (GC-MS/FID) and two-dimensional gas
74 chromatography techniques (GC×GC) (Alam et al., 2018; Alam et al., 2016; de Gouw
75 et al., 2017; Liang et al., 2018; Zhao et al., 2016). Based on measurements of gas
76 chromatographic techniques, the signals of unresolved cyclic compounds can be
77 determined from subtracting the total signal for each retention time bin according to the
78 series of *n*-alkanes (Zhao et al., 2014; Zhao et al., 2016). The mass of linear alkanes and
79 branched alkanes in each bin is calculated by using the total ion current (TIC) and the
80 fraction of characteristic fragments ($C_4H_9^+$, m/z 57) (Zhao et al., 2014; Zhao et al.,
81 2016). However, this type of quantitative method does not explicitly distinguish
82 individual cycloalkanes, and the determined mass may contain other cyclic compounds,
83 e.g., polycyclic aromatic hydrocarbons and compounds containing oxygen or
84 multifunctional groups (Zhao et al., 2014; Zhao et al., 2015; Zhao et al., 2016). Due to
85 the need for collection and pretreatment of air samples, time resolution of GC-MS
86 techniques is usually in the range of 0.5-1.0 h or above.

87 Proton transfer reaction mass spectrometer (PTR-MS) using hydronium ions
88 (H_3O^+) as the reagent ion, is capable for measuring many organic compounds with high
89 response time and sensitivity (de Gouw and Warneke, 2007; Yuan et al., 2017).
90 However, detection of alkanes and cycloalkanes using PTR-MS with H_3O^+ ionization
91 is challenging, as usually only a series of fragment ions ($C_nH_{2n+1}^+$, $C_nH_{2n-1}^+$, $n \geq 3$) are
92 observed (Erickson et al., 2014; Gueneron et al., 2015). Recently, it was demonstrated
93 that linear alkanes can be measured by PTR-MS with time-of-flight detector using NO^+
94 as reagent ions (NO^+ PTR-ToF-MS) (Inomata et al., 2014; Koss et al., 2016; Wang et
95 al., 2020). These higher alkanes are ionized by NO^+ via hydride ion transfer leading to
96 major product ions of $C_nH_{2n+1}^+$, with low degree of fragmentation (Inomata et al., 2014).



97 Meanwhile, it is interesting that cycloalkanes were also tried to be quantified using
98 $C_nH_{2n+1}^+$ ions in H_3O^+ PTR-MS in oil and gas regions (Koss et al., 2017; Warneke et
99 al., 2014; Yuan et al., 2014), though sensitivities were substantially low (~10% of other
100 species) (Warneke et al., 2014). These evidences suggest that NO^+ ionization scheme
101 could provide a possibility for measuring cycloalkanes along with acyclic alkanes, as
102 demonstrated in a recent laboratory chamber work (Wang et al., 2022a).

103 In this study, we discuss the potential of online measurements of cycloalkanes in
104 ambient air and form emission sources utilizing NO^+ ionization in PTR-ToF-MS. The
105 results of laboratory experiments of characterization of product ions, calibration, and
106 response time will be shown. Finally, measurements of cycloalkanes using NO^+ PTR-
107 ToF-MS will be demonstrated from deployments at an urban site in southern China and
108 a chassis dynamometer study for vehicular emissions.

109 2 Methods

110 2.1 NO^+ PTR-ToF-MS measurements

111 A commercially PTR-ToF-MS instrument (Ionicon Analytik, Austria) equipped
112 with a quadrupole ion (Qi) guide for effective transfer of ions from drift tube to the
113 time-of-flight mass spectrometer is used for this work (Sulzer et al., 2014), and the mass
114 resolving approximately reach about $3000\text{ m}/\Delta\text{m}$ (Fig. S1). In order to generate NO^+
115 ions, 5 sccm ultra-high-purity air ($O_2+N_2\geq 99.999\%$) is directed into to the hollow
116 cathode discharge area of ion source, NO^+ ions are produced by ionization as follows
117 (Federer et al., 1985):



119 For the purpose of ionize NO^+ ions to the greatest extent, reduce the generation of
120 impurity ions such as H_3O^+ , O_2^+ and NO_2^+ , the ion source voltage U_s and U_{s0} were set
121 to 40 V and 100 V ,while drift tube voltages U_{dx} and U_{drift} were set to 23.5 V and 470
122 V with drift tube pressure at 3.8 mbar, resulting in an E/N (electric potential intensity
123 relative to gas number density) of 60 Td (Wang et al., 2020). The measured ToF data is



124 processed for high-resolution peak fitting using Tofware (Tofwerk AG, version, 3.0.3),
125 obtaining high precision signals for cycloalkanes (Fig. S2). A description of the fitting
126 and calculation methods are fully discussed in previous studies (Stark et al., 2015;
127 Timonen et al., 2016). The raw ion count signals of NO^+ PTR-ToF-MS are normalized
128 to the primary ion (NO^+) at a level of 10^6 cps to account for fluctuations of ion source
129 and detector (see SI).

130 Compared to proton transfer reactions between H_3O^+ ions and VOCs species, NO^+
131 ions show a variety of reaction pathways with VOCs, which can be roughly summarized
132 as follow:

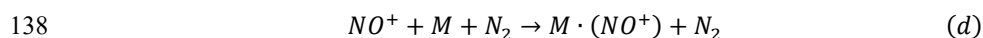
133 charge transfer:



135 hydride ion transfer:



137 association reaction:



139 As shown in Fig. 1, the ionization energy (IE) of VOC species is a determination
140 factor for the reaction pathways with NO^+ . For example, as the IE of NO is 9.26 eV
141 (Reiser et al., 1988), species with IE less than 9.26 eV, e.g., benzene and isoprene, will
142 undergo charge transfer reaction (b) with NO^+ (Španěl and Smith, 1999, 1996), while
143 species with IE greater than 9.26 eV, e.g., acetone and *n*-undecane, will undergo hydride
144 ion transfer (c) or association reaction (d) with NO^+ (Amador-Muñoz et al., 2016;
145 Diskin et al., 2002; Koss et al., 2016).

146 **2.2 Calibration and correction experiments**

147 In this study, we investigate characteristic ions of cycloalkanes produced undergo
148 the NO^+ ionization from a series of species identification experiments. The information
149 of cycloalkanes chemicals used in these experiments is listed in Table 1. In addition, we
150 also evaluated potential interferences from mono-alkenes, the isomers of cycloalkanes.
151 Calibration experiments were carried out to obtain sensitivities of cycloalkanes in both



152 the laboratory and the field, using a customized cylinder gas standard (Apel-Riemer
153 Environmental, Inc. USA), containing five different alkyl-cyclohexanes (C₁₀-C₁₄) and
154 eight *n*-alkanes (C₈-C₁₅) (Table S1).

155 Furthermore, some additional experiments were performed to explore the
156 influences of humidity and tubing delay effects on measurements of cycloalkanes.
157 Previously, it was shown that response factors of higher alkanes in NO⁺ PTR-ToF-MS
158 are slightly affected by air humidity, and the degree of influence is related to carbon
159 number (Wang et al., 2020). Therefore, we evaluate the influence of humidity on
160 sensitivity of cycloalkanes in NO⁺ PTR-ToF-MS using a custom-built humidity
161 delivery system (Fig. S3), and the results are applied to explore the relationship between
162 sensitivities of cycloalkanes and humidity. The perfluoroalkoxy (PFA) Teflon tubing is
163 used for inlets in this study, but gas-wall partitioning can be important for low volatility
164 compounds (Pagonis et al., 2017). As the result, measurements from controlled
165 laboratory experiments and field deployments were analyzed to systematically quantify
166 and characterize tubing delay time of cycloalkanes.

167 **3 Results and discussion**

168 **3.1 Characterization of product ion distribution**

169 NO⁺ PTR-ToF-MS was used to directly measure high-purity cycloalkane
170 chemicals and identify the characteristic product ions produced by cycloalkanes under
171 NO⁺ ionization. Here, the major product ions, fragments and their contributions for
172 different cycloalkanes are shown in Table 1. Chemical formulas of the product ions are
173 determined based on the positions of measured mass peaks.

174 Fig. 2 shows mass spectra within the relevant range (m/z 60⁺ to 200⁺ Th) for
175 cycloalkanes. The signals are normalized to the largest ion peak for better comparison.
176 As shown in Fig. 2, no significant fragmentation appears for cycloheptane and
177 methylcyclohexane (C₇H₁₄), and the dominating product ions are observed at m/z 97
178 Th, corresponding to C₇H₁₃⁺. Similarly, the product ions generated by



179 hexylcyclohexane and cyclododecane ($C_{12}H_{24}$) under NO^+ ionization mainly appear at
180 m/z 167 Th (Fig. 2c-d), corresponding to $C_{12}H_{23}^+$, and fragments occurred at m/z 97 Th
181 and m/z 111 Th, corresponding to $C_7H_{13}^+$ and $C_8H_{15}^+$, respectively. Bicyclic
182 cycloalkanes undergo the same ionization channel from NO^+ ionization, as
183 demonstrated by major product ions at m/z 165 Th ($C_{12}H_{21}^+$) and other fragmentation
184 ions from bicyclohexyl ($C_{12}H_{22}$) (Fig. 2e). These results verify that reactions of cyclic
185 and bicyclic alkanes with NO^+ ions follow the hydride ion transfer pathway to yield
186 $C_nH_{2n-1}^+$ and $C_nH_{2n-3}^+$ product ions, respectively. As mentioned above, the characteristic
187 peaks of cycloalkanes under NO^+ ionization is consistent with the ions for attempts to
188 utilize H_3O^+ PTR-MS for cycloalkanes detection in previous studies, though with low
189 sensitivities reported for cycloalkanes (Erickson et al., 2014; Gueneron et al., 2015;
190 Warneke et al., 2014; Yuan et al., 2014). As the result, we speculate that reactions of
191 NO^+ with cycloalkanes may present large contributions to cycloalkane M-H product
192 ions in the H_3O^+ chemistry mode of PTR-MS (Španěl et al., 1995).

193 As the isomers of cyclic alkanes, alkenes may interfere with measurements of
194 cycloalkanes. Here, we use 1-heptene (C_7H_{14}) and 1-decene ($C_{10}H_{20}$), isomers of C_7 and
195 C_{10} cyclic alkanes, to explore the ionization regime of alkenes in NO^+ chemical
196 ionization (Fig. 3 and Table 1). These two alkenes produce more fragments than
197 cycloalkanes under NO^+ chemistry, but mainly react with NO^+ via association reaction
198 to yield $C_nH_{2n} \cdot (NO)^+$ product ions. The major product ions of 1-heptene and 1-decene
199 appear at m/z 128 Th and m/z 170 Th, corresponding to $C_7H_{13}HNO^+$ and $C_{10}H_{19}HNO^+$,
200 respectively. Based on the mass spectra, alkenes produce the $C_nH_{2n-1}^+$ product ions at
201 fractions of $<5\%$, which are similar to NO^+ ionization results of the two species and
202 other 1-alkenes determined from a selected ion flow tube mass spectrometer (SIFT-MS)
203 (Diskin et al., 2002). The same study (Diskin et al., 2002) also demonstrated that trans-
204 2-alkenes might produce more $C_nH_{2n-1}^+$ ions under NO^+ ionization (e.g., trans-2-
205 heptene contributions 40% of $C_7H_{13}^+$ ions). However, concentrations of 1-alkenes and
206 trans-2-alkenes in the atmosphere are usually significantly lower than cycloalkanes



207 (about 25% and <5%, respectively) (de Gouw et al., 2017; Yuan et al., 2013). Therefore,
208 we conclude the interferences of alkenes on measurements of cycloalkanes in most
209 environments are small.

210 **3.2 Sensitivity, humidity dependence and detection limits**

211 The calibration experiments of cycloalkanes are carried out in both dry conditions
212 (<1% RH) and humidified conditions (Fig. S5). Fig. 4 illustrates results from a typical
213 calibration experiment for five different alkyl-substituted cyclohexanes with carbon
214 atoms of 10-14 in dry air (relative humidity < 1%) for NO⁺ PTR-ToF-MS. There is a
215 good linear relationship between ion signals and concentrations of various cycloalkanes
216 ($R=0.9996-0.9999$). Sensitivities (ncps ppb⁻¹) of cycloalkanes are in the range of 210 to
217 260 ncps ppb⁻¹ (Table 2). The sensitivity of each cycloalkanes remained stable in the
218 long-term calibration conducted in the laboratory and in the field (Fig. S6). Table 2
219 further shows detection limits of cycloalkanes by NO⁺ PTR-ToF-MS, which are
220 calculated as the concentrations with the signal-to-noise ratio of 3 (Bertram et al., 2011;
221 Yuan et al., 2017). The detection limits of cycloalkanes at integral time of 10 s and 1
222 min are in the range of 6.2 to 8.2 ppt and 2.4-3.6 ppt, respectively. For comparison, the
223 detection limits of NO⁺ PTR-ToF-MS for 24 h of integral time are also determined,
224 obtaining comparable results (<0.1 ppt) with detection limits of GC×GC-ToF-MS (0.1-
225 0.3 ppt for daily sample) (Liang et al., 2018; Xu et al., 2020a),.

226 Fig. 4b shows that normalized signals of hexylcyclohexane relative to dry
227 conditions as a function of different humidity. The relative signals of the explored
228 cycloalkanes show minor decrease (<10%) at the highest humidity (~82% RH at 25°C)
229 compare to dry condition, and the observed changes for cycloalkanes with different
230 carbon number are similar, suggesting little influence of humidity on measurements of
231 cycloalkanes. The humidity-dependence curves determined in Fig. 4b are used to
232 corrected variations of ambient humidity in the atmosphere.

233 The response time of various cycloalkanes in the instrument and also sampling
234 tubing is determined from laboratory experiments (Fig. S6). For the species not in the



235 gas standard, we also take advantage of vehicular emissions measurements associated
236 with high concentrations of cycloalkanes. Here, we use the delay time to determine
237 response of cycloalkanes, which is calculated based on the time it takes for signals to
238 drop to 10% of its initial value (Fig. S7) (Pagonis et al., 2017). The delay time of
239 cycloalkanes are summarized in Fig. 5. The delay time of various cycloalkanes
240 generally increases with the carbon numbers, ranging from a few seconds to a few
241 minutes, but relatively lower than those acyclic alkanes within C₁₀-C₁₅ range (Wang et
242 al., 2020). These results suggest that measured variability of cycloalkanes with higher
243 carbon number, especially for C₁₉-C₂₀ or above, may only be reliable for time scales
244 longer than 10 min.

245 **3.3 Applications in ambient air and vehicular exhausts**

246 Based on the results shown above, we deployed the NO⁺ PTR-ToF-MS to measure
247 concentration levels and variations of cycloalkanes at an urban site in Guangzhou,
248 southern China. Details of the field campaign were described in previous studies (Wang
249 et al., 2020; Wu et al., 2020). The average sensitivities of long-term calibration (dry
250 condition) during the field observations were used to quantify cycloalkanes after
251 corrected variations of ambient humidity in the atmosphere. For the cycloalkanes that
252 are not contained in the gas standard, we employ average sensitivity for calibrated
253 cycloalkanes in gas standard.

254 The concentration levels and diurnal profiles of cyclic and bicyclic alkanes are
255 illustrated in Fig. 6a, along with CO. In general, cyclic and bicyclic alkanes
256 demonstrated similar temporal variability as CO, suggesting cyclic and bicyclic alkanes
257 may be mainly emitted from primary combustion sources. Concentrations of C₁₂
258 bicyclic alkanes are observed to be comparable with C₁₂ cyclic alkanes. As shown in
259 Fig. 6b, selected C₁₀ and C₁₂ cycloalkanes show diurnal variations with lower
260 concentration during the daytime. Compared to diurnal variations of other species with
261 different reactivity (Wu et al., 2020), the decline fractions of cycloalkanes are more
262 comparable to reactive species (e.g., C₈ aromatics) than the inert ones (e.g., CO,



263 benzene), indicating significantly daytime photochemical removal of these
264 cycloalkanes. Diurnal patterns of other cyclic and bicyclic alkanes exhibit similar
265 results (Fig. S8). As discussed in Wang et al. (2020), similar diurnal profiles of
266 cycloalkanes with different carbon number also imply that tubing-delay effect may not
267 affect significantly to temporal variations of cycloalkanes reported here. Based on both
268 time series and correlation analysis (Fig. 6c), cyclic and bicyclic alkanes showed strong
269 correlation with acyclic alkanes, suggesting they came from same emission sources.

270 NO^+ PTR-ToF-MS was also applied to measure cycloalkanes emissions along with
271 other organic compounds from vehicles using gasoline, diesel, and LPG as fuel, by
272 conducting a chassis dynamometer measurement (Wang et al., 2022b). Fig. 7 shows
273 time series of C_{12} cyclic and bicyclic alkanes, C_{12} alkanes, toluene, and acetaldehyde
274 measured by NO^+ PTR-ToF-MS for a gasoline vehicle with emission standard of China
275 III and a diesel vehicle with emission standard of China IV. Both test vehicles were
276 started with hot engines. As shown in Fig. 7a, high concentrations of selected
277 cycloalkanes emitted by the gasoline vehicle were observed as the engine started.
278 Compared with typical VOC compounds exhausted by vehicles (e.g., toluene and
279 acetaldehyde), concentrations of cycloalkanes were lower but showed similar temporal
280 variations. In comparison, cycloalkanes emissions from diesel vehicles are obviously
281 different. As shown in Fig. 7b, concentrations of cycloalkanes showed relatively
282 moderate enhancements as engine started, but significantly enhanced with high vehicle
283 speed, obtaining periodic pattern variations within each test cycle. Though the highest
284 concentrations of cycloalkanes observed for gasoline and diesel vehicles are similar,
285 determined emission factors of diesel vehicles are significantly larger than gasoline
286 vehicles, since emissions of cycloalkanes are mainly concentrated during a short period
287 at engine start for gasoline vehicles, whereas emissions of cycloalkanes remain high
288 during hot running for diesel vehicles. For instance, the determined emission factors of
289 C_{12} cyclic alkanes are 0.06 mg km^{-1} for gasoline vehicle and 1.17 mg km^{-1} for diesel
290 vehicles, respectively. Recent studies reported that cyclic compounds occupied a large



291 proportion in IVOCs emitted from vehicles, with prominent SOA formation potentials
292 (Fang et al., 2021; Huang et al., 2018; Zhao et al., 2016), but emissions of individual
293 cycloalkanes were not reported yet. As the result, high time-resolution measurements
294 of cycloalkanes from vehicular emissions by NO^+ PTR-ToF-MS can improve the
295 characterization of emission mechanisms of these species.

296 **3.4 Insights from simultaneous measurements of cycloalkanes and** 297 **alkanes**

298 Since NO^+ PTR-ToF-MS can provide simultaneous measurements of cycloalkanes
299 and acyclic alkanes, we can use this information to explore the relative importance of
300 cycloalkanes. Fig. 8 shows mean concentrations of cycloalkanes (cyclic and bicyclic)
301 and alkanes with different carbon numbers ($\text{C}_{10}\text{-C}_{20}$) measured by NO^+ PTR-ToF-MS
302 in urban air and emissions from diesel vehicles. In urban region, concentrations of
303 cyclic and bicyclic cycloalkanes are comparable, but lower than acyclic alkanes, with
304 concentration ratios relative to acyclic alkanes in the range of 0.30-0.46 for cyclic
305 alkanes and 0.23-0.51 for bicyclic alkanes. Similar results are obtained for gasoline
306 vehicles, with cyclic alkanes/acyclic alkanes and bicyclic alkanes/acyclic ratios of 0.27-
307 0.53 for and 0.21-0.52, respectively (Fig. 9). The contributions of cycloalkanes in diesel
308 vehicular emissions are relatively higher, with the concentration ratios relative to
309 acyclic alkanes in the range of 0.42-0.66 for cyclic alkanes and 0.37-0.95 for bicyclic
310 alkanes.

311 As there is only limited measurements of bicyclic alkanes in the literature, we
312 compare concentration ratios of cyclic alkanes to acyclic alkanes with results in
313 previous studies, mainly determined from measurements by GC-MS/FID and GC \times GC.
314 As shown in the Fig. 9, the ratios obtained in the urban region of Guangzhou in this
315 work (0.2-0.4) are similar to other measurements in urban area, including London, UK
316 (Xu et al., 2020b) and Algiers, Algeria (Yassaa et al., 2001). As for emissions from
317 diesel vehicles, the ratios measured in this study are similar to GC \times GC measurements
318 in UK (Alam et al., 2016) for $\text{C}_{12}\text{-C}_{14}$ range, whereas the ratios from this study are



319 higher than Alam et al. (2016) for larger carbon number. The relative fractions of
320 cycloalkanes measured from oil and gas region (Gilman et al., 2013) and emissions
321 from lubricating oil (Liang et al., 2018) (>0.7) are relatively higher than ambient air
322 and vehicular emissions. The variability pattern of cyclic alkanes to acyclic alkanes
323 ratios for different carbon number may be used for source analysis of these IVOCs in
324 the future.

325 **4 Conclusion**

326 In this study, we show that online measurements of cycloalkanes can be achieved
327 using proton transfer reaction time-of-flight mass spectrometry with NO^+ chemical
328 ionization (NO^+ PTR-ToF-MS). Our results demonstrate that cyclic and bicyclic
329 alkanes are ionized via hydride ion transfer leading to characteristic product ions of
330 $\text{C}_n\text{H}_{2n-1}^+$ and $\text{C}_n\text{H}_{2n-3}^+$, respectively. As isomers of cycloalkanes, alkenes undergoes
331 association reactions mainly yielding product ions $\text{C}_n\text{H}_{2n}\cdot(\text{NO})^+$, which induce little
332 interference to cycloalkanes detection. Calibration of various cycloalkanes show
333 similar sensitivities with small humidity dependence. The detection limits of
334 cycloalkanes are in the range of 2-4 ppt at integral time of 1 min.

335 Applying this method, cycloalkanes were successfully measured at an urban site
336 in southern China and a chassis dynamometer study for vehicular emissions.
337 Concentrations of both cyclic and bicyclic alkanes are substantial in urban air and
338 vehicular emissions. Diurnal variations of cycloalkanes in the urban air indicate
339 significant losses due to photochemical processes during the daytime. The
340 concentration ratios of cyclic alkanes to acyclic alkanes are similar between urban air
341 and gasoline vehicle emissions, but higher for diesel vehicles, which could be
342 potentially used for source analysis in future studies. Our work demonstrates that NO^+
343 PTR-ToF-MS provides a new complementary approach for fast characterization of
344 cycloalkanes in both ambient air and emission sources, which can be helpful to
345 investigate sources of cycloalkanes and their contribution to SOA formation in the



346 atmosphere. Measurements of cycloalkanes in the particle phase may also be possible
347 by combining NO^+ PTR-ToF-MS with “chemical analysis of aerosols online”
348 (CHARON) or other similar aerosol inlets (Muller et al., 2017), which could further
349 provide particle-phase information of cycloalkanes and gas-partitioning analysis of
350 cycloalkanes.

351

352 **Data availability**

353 Data are available from the authors upon request.

354 **Author contribution**

355 BY designed the research. YBC, CMW, SHW, XJH, CHW, XS, YBH, XBL, YJL
356 and MS contributed to data collection. YBC performed data analysis, with contributions
357 from CMW, SHW, XJH, and CHW. YBC and BY prepared the manuscript with
358 contributions from other authors. All the authors reviewed the manuscript.

359 **Competing interests**

360 The authors declare that they have no known competing financial interests or
361 personal relationships that could have appeared to influence the work reported in this
362 paper.

363 **Acknowledgement**

364 This work was supported by the National Natural Science Foundation of China
365 (grant No. 41877302, 42121004), Key-Area Research and Development Program of
366 Guangdong Province (grant No. 2020B1111360003), and Guangdong Innovative and
367 Entrepreneurial Research Team Program (grant No. 2016ZT06N263). This work was
368 also supported by Special Fund Project for Science and Technology Innovation Strategy
369 of Guangdong Province (Grant No.2019B121205004).

370 **Reference**

371 Aklilu, Y.-a., Cho, S., Zhang, Q., and Taylor, E.: Source apportionment of volatile
372 organic compounds measured near a cold heavy oil production area, Atmospheric



- 373 Research, 206, 75-86, 2018.
- 374 Alam, M. S., Zeraati-Rezaei, S., Liang, Z., Stark, C., Xu, H., Mackenzie, A. R.,
375 and Harrison, R. M.: Mapping and quantifying isomer sets of hydrocarbons ($\geq C_{12}$)
376 in diesel exhaust, lubricating oil and diesel fuel samples using GC \times GC-ToF-MS,
377 Atmospheric Measurement Techniques, 11, 3047-3058, 2018.
- 378 Alam, M. S., Zeraati-Rezaei, S., Stark, C. P., Liang, Z., Xu, H., and Harrison, R.
379 M.: The characterisation of diesel exhaust particles – composition, size distribution and
380 partitioning, Faraday Discussions, 189, 69-84, 2016.
- 381 Amador-Muñoz, O., Misztal, P. K., Weber, R., Worton, D. R., Zhang, H., Drozd,
382 G., and Goldstein, A. H.: Sensitive detection of *n*-alkanes using a mixed ionization
383 mode proton-transfer-reaction mass spectrometer, Atmospheric Measurement
384 Techniques, 9, 5315-5329, 2016.
- 385 Bertram, T. H., Kimmel, J. R., Crisp, T. A., Ryder, O. S., Yatavelli, R. L. N.,
386 Thornton, J. A., Cubison, M. J., Gonin, M., and Worsnop, D. R.: A field-deployable,
387 chemical ionization time-of-flight mass spectrometer, Atmospheric Measurement
388 Techniques, 4, 1471-1479, 2011.
- 389 de Gouw, J. and Warneke, C.: Measurements of volatile organic compounds in the
390 earth's atmosphere using proton-transfer-reaction mass spectrometry, Mass Spectrom
391 Rev, 26, 223-257, 2007.
- 392 de Gouw, J. A.: Budget of organic carbon in a polluted atmosphere: Results from
393 the New England Air Quality Study in 2002, Journal of Geophysical Research, 110,
394 2005.
- 395 de Gouw, J. A., Gilman, J. B., Kim, S. W., Lerner, B. M., Isaacman-VanWertz, G.,
396 McDonald, B. C., Warneke, C., Kuster, W. C., Lefer, B. L., Griffith, S. M., Dusanter,
397 S., Stevens, P. S., and Stutz, J.: Chemistry of Volatile Organic Compounds in the Los
398 Angeles basin: Nighttime Removal of Alkenes and Determination of Emission Ratios,
399 Journal of Geophysical Research: Atmospheres, 122, 11,843-811,861, 2017.
- 400 Diskin, A. M., Wang, T. S., Smith, D., and Spanel, P.: A selected ion flow tube



401 (SIFT), study of the reactions of H_3O^+ , NO^+ and O_2^+ ions with a series of alkenes; in
402 support of SIFT-MS, *International Journal of Mass Spectrometry*, 218, 87-101, 2002.

403 Donahue, N. M., Kroll, J. H., Pandis, S. N., and Robinson, A. L.: A two-
404 dimensional volatility basis set - Part 2: Diagnostics of organic-aerosol evolution,
405 *Atmospheric Chemistry and Physics*, 12, 615-634, 2012.

406 Erickson, M. H., Gueneron, M., and Jobson, B. T.: Measuring long chain alkanes
407 in diesel engine exhaust by thermal desorption PTR-MS, *Atmospheric Measurement*
408 *Techniques*, 7, 225-239, 2014.

409 Fang, H., Huang, X., Zhang, Y., Pei, C., Huang, Z., Wang, Y., Chen, Y., Yan, J.,
410 Zeng, J., Xiao, S., Luo, S., Li, S., Wang, J., Zhu, M., Fu, X., Wu, Z., Zhang, R., Song,
411 W., Zhang, G., Hu, W., Tang, M., Ding, X., Bi, X., and Wang, X.: Measurement report:
412 Emissions of intermediate-volatility organic compounds from vehicles under real-
413 world driving conditions in an urban tunnel, *Atmospheric Chemistry and Physics*, 21,
414 10005-10013, 2021.

415 Federer, W., Dobler, W., Howorka, F., Lindinger, W., Durup - Ferguson, M., and
416 Ferguson, E. E.: Collisional relaxation of vibrationally excited $\text{NO}^+(v)$ ions, *The Journal*
417 *of Chemical Physics*, 83, 1032-1038, 1985.

418 Gilman, J. B., Lerner, B. M., Kuster, W. C., and de Gouw, J. A.: Source Signature
419 of Volatile Organic Compounds from Oil and Natural Gas Operations in Northeastern
420 Colorado, *Environmental Science & Technology*, 47, 1297-1305, 2013.

421 Goldstein, A. H. and Galbally, I. E.: Known and unknown organic constituents in
422 the Earth' s atmosphere, *Environmental Science & Technology*, 41, 1514-1521, 2007.

423 Gueneron, M., Erickson, M. H., VanderSchelden, G. S., and Jobson, B. T.: PTR-
424 MS fragmentation patterns of gasoline hydrocarbons, *International Journal of Mass*
425 *Spectrometry*, 379, 97-109, 2015.

426 He, X., Yuan, B., Wu, C., Wang, S., Wang, C., Huangfu, Y., Qi, J., Ma, N., Xu, W.,
427 Wang, M., Chen, W., Su, H., Cheng, Y., and Shao, M.: Volatile organic compounds in
428 wintertime North China Plain: Insights from measurements of proton transfer reaction



429 time-of-flight mass spectrometer (PTR-ToF-MS), *Journal of Environmental Sciences*,
430 114, 98-114, 2022.

431 Hu, W., Zhou, H., Chen, W., Ye, Y., Pan, T., Wang, Y., Song, W., Zhang, H., Deng,
432 W., Zhu, M., Wang, C., Wu, C., Ye, C., Wang, Z., Yuan, B., Huang, S., Shao, M., Peng,
433 Z., Day, D. A., Campuzano-Jost, P., Lambe, A. T., Worsnop, D. R., Jimenez, J. L., and
434 Wang, X.: Oxidation Flow Reactor Results in a Chinese Megacity Emphasize the
435 Important Contribution of S/IVOCs to Ambient SOA Formation, *Environmental*
436 *Science & Technology*, 56, 6880-6893, 2022.

437 Huang, C., Hu, Q., Li, Y., Tian, J., Ma, Y., Zhao, Y., Feng, J., An, J., Qiao, L., Wang,
438 H., Jing, S. A., Huang, D., Lou, S., Zhou, M., Zhu, S., Tao, S., and Li, L.: Intermediate
439 Volatility Organic Compound Emissions from a Large Cargo Vessel Operated under
440 Real-World Conditions, *Environmental Science & Technology*, 52, 12934-12942, 2018.

441 Hunter, J. F., Carrasquillo, A. J., Daumit, K. E., and Kroll, J. H.: Secondary organic
442 aerosol formation from acyclic, monocyclic, and polycyclic alkanes, *Environmental*
443 *Science & Technology*, 48, 10227-10234, 2014.

444 Inomata, S., Tanimoto, H., and Yamada, H.: Mass Spectrometric Detection of
445 Alkanes Using NO⁺ Chemical Ionization in Proton-transfer-reaction Plus Switchable
446 Reagent Ion Mass Spectrometry, *Chemistry Letters*, 43, 538-540, 2014.

447 Jahn, L. G., Wang, D. S., Dhulipala, S. V., and Ruiz, L. H.: Gas-Phase Chlorine
448 Radical Oxidation of Alkanes: Effects of Structural Branching, NO_x, and Relative
449 Humidity Observed during Environmental Chamber Experiments, *The Journal of*
450 *Physical Chemistry A*, 125, 7303-7317, 2021.

451 Koss, A., Yuan, B., Warneke, C., Gilman, J. B., Lerner, B. M., Veres, P. R., Peischl,
452 J., Eilerman, S., Wild, R., Brown, S. S., Thompson, C. R., Ryerson, T., Hanisco, T.,
453 Wolfe, G. M., Clair, J. M. S., Thayer, M., Keutsch, F. N., Murphy, S., and de Gouw, J.:
454 Observations of VOC emissions and photochemical products over US oil- and gas-
455 producing regions using high-resolution H₃O⁺ CIMS (PTR-ToF-MS), *Atmospheric*
456 *Measurement Techniques*, 10, 2941-2968, 2017.



- 457 Koss, A. R., Warneke, C., Yuan, B., Coggon, M. M., Veres, P. R., and de Gouw, J.
458 A.: Evaluation of NO^+ reagent ion chemistry for online measurements of atmospheric
459 volatile organic compounds, *Atmospheric Measurement Techniques*, 9, 2909-2925,
460 2016.
- 461 Li, J., Wang, W., Li, K., Zhang, W., Peng, C., Liu, M., Chen, Y., Zhou, L., Li, H.,
462 and Ge, M.: Effect of chemical structure on optical properties of secondary organic
463 aerosols derived from C12 alkanes, *Science of The Total Environment*, 751, 141620,
464 2021.
- 465 Li, Y., Ren, B., Qiao, Z., Zhu, J., Wang, H., Zhou, M., Qiao, L., Lou, S., Jing, S.,
466 Huang, C., Tao, S., Rao, P., and Li, J.: Characteristics of atmospheric intermediate
467 volatility organic compounds (IVOCs) in winter and summer under different air
468 pollution levels, *Atmospheric Environment*, 210, 58-65, 2019.
- 469 Liang, Z., Chen, L., Alam, M. S., Zeraati Rezaei, S., Stark, C., Xu, H., and Harrison,
470 R. M.: Comprehensive chemical characterization of lubricating oils used in modern
471 vehicular engines utilizing GC \times GC-TOFMS, *Fuel*, 220, 792-799, 2018.
- 472 Lim, Y. B. and Ziemann, P. J.: Effects of Molecular Structure on Aerosol Yields
473 from OH Radical-Initiated Reactions of Linear, Branched, and Cyclic Alkanes in the
474 Presence of NO_x , *Environmental Science & Technology*, 43, 2328-2334, 2009.
- 475 Lou, H., Hao, Y., Zhang, W., Su, P., Zhang, F., Chen, Y., Feng, D., and Li, Y.:
476 Emission of intermediate volatility organic compounds from a ship main engine
477 burning heavy fuel oil, *Journal of Environmental Sciences*, 84, 197-204, 2019.
- 478 Loza, C. L., Craven, J. S., Yee, L. D., Coggon, M. M., Schwantes, R. H., Shiraiwa,
479 M., Zhang, X., Schilling, K. A., Ng, N. L., Canagaratna, M. R., Ziemann, P. J., Flagan,
480 R. C., and Seinfeld, J. H.: Secondary organic aerosol yields of 12-carbon alkanes,
481 *Atmospheric Chemistry and Physics*, 14, 1423-1439, 2014.
- 482 Monks, P. S., Archibald, A. T., Colette, A., Cooper, O., Coyle, M., Derwent, R.,
483 Fowler, D., Granier, C., Law, K. S., Mills, G. E., Stevenson, D. S., Tarasova, O., Thouret,
484 V., von Schneidmesser, E., Sommariva, R., Wild, O., and Williams, M. L.:



485 Tropospheric ozone and its precursors from the urban to the global scale from air quality
486 to short-lived climate forcer, *Atmospheric Chemistry and Physics*, 15, 8889-8973, 2015.

487 Muller, M., Eichler, P., D'Anna, B., Tan, W., and Wisthaler, A.: Direct Sampling
488 and Analysis of Atmospheric Particulate Organic Matter by Proton-Transfer-Reaction
489 Mass Spectrometry, *Anal Chem*, 89, 10889-10897, 2017.

490 Pagonis, D., Krechmer, J. E., de Gouw, J., Jimenez, J. L., and Ziemann, P. J.:
491 Effects of gas-wall partitioning in Teflon tubing and instrumentation on time-resolved
492 measurements of gas-phase organic compounds, *Atmospheric Measurement
493 Techniques*, 10, 4687-4696, 2017.

494 Reiser, G., Habenicht, W., Müller-Dethlefs, K., and Schlag, E. W.: The ionization
495 energy of nitric oxide, *Chemical Physics Letters*, 152, 119-123, 1988.

496 Robinson, A. L., Donahue, N. M., Shrivastava, M. K., Weitkamp, E. A., Sage, A.
497 M., Grieshop, A. P., Lane, T. E., Pierce, J. R., and Pandis, S. N.: Rethinking Organic
498 Aerosols: Semivolatile Emissions and Photochemical Aging, *Science*, 315, 1259-1262,
499 2007.

500 Španěl, P., Pavlik, M., and Smith, D.: Reactions of H_3O^+ and OH^- ions with some
501 organic molecules; applications to trace gas analysis in air, *International Journal of
502 Mass Spectrometry and Ion Processes*, 145, 177-186, 1995.

503 Španěl, P. and Smith, D.: Selected ion flow tube studies of the reactions of H_3O^+ ,
504 NO^+ , and O_2^+ with several aromatic and aliphatic monosubstituted halocarbons,
505 *International Journal of Mass Spectrometry*, 189, 213-223, 1999.

506 Španěl, P. and Smith, D.: A selected ion flow tube study of the reactions of NO^+ and
507 O_2^+ ions with some organic molecules: The potential for trace gas analysis of air, *The
508 Journal of Chemical Physics*, 104, 1893-1899, 1996.

509 Stark, H., Yatavelli, R. L. N., Thompson, S. L., Kimmel, J. R., Cubison, M. J.,
510 Chhabra, P. S., Canagaratna, M. R., Jayne, J. T., Worsnop, D. R., and Jimenez, J. L.:
511 Methods to extract molecular and bulk chemical information from series of complex
512 mass spectra with limited mass resolution, *International Journal of Mass Spectrometry*,



- 513 389, 26-38, 2015.
- 514 Sulzer, P., Hartungen, E., Hanel, G., Feil, S., Winkler, K., Mutschlechner, P.,
515 Haidacher, S., Schottkowsky, R., Gunsch, D., Seehauser, H., Striednig, M., Jürschik, S.,
516 Breiev, K., Lanza, M., Herbig, J., Märk, L., Märk, T. D., and Jordan, A.: A Proton
517 Transfer Reaction-Quadrupole interface Time-Of-Flight Mass Spectrometer (PTR-
518 QiTOF): High speed due to extreme sensitivity, *International Journal of Mass*
519 *Spectrometry*, 368, 1-5, 2014.
- 520 Timonen, H., Cubison, M., Aurela, M., Brus, D., Lihavainen, H., Hillamo, R.,
521 Canagaratna, M., Nekat, B., Weller, R., Worsnop, D., and Saarikoski, S.: Applications
522 and limitations of constrained high-resolution peak fitting on low resolving power mass
523 spectra from the ToF-ACSM, *Atmospheric Measurement Techniques*, 9, 3263-3281,
524 2016.
- 525 Tkacik, D. S., Presto, A. A., Donahue, N. M., and Robinson, A. L.: Secondary
526 Organic Aerosol Formation from Intermediate-Volatility Organic Compounds: Cyclic,
527 Linear, and Branched Alkanes, *Environmental Science & Technology*, 46, 8773-8781,
528 2012.
- 529 Wang, C. M., Yuan, B., Wu, C. H., Wang, S. H., Qi, J. P., Wang, B. L., Wang, Z.
530 L., Hu, W. W., Chen, W., Ye, C. S., Wang, W. J., Sun, Y. L., Wang, C., Huang, S., Song,
531 W., Wang, X. M., Yang, S. X., Zhang, S. Y., Xu, W. Y., Ma, N., Zhang, Z. Y., Jiang, B.,
532 Su, H., Cheng, Y. F., Wang, X. M., and Shao, M.: Measurements of higher alkanes using
533 NO⁺ chemical ionization in PTR-ToF-MS: important contributions of higher alkanes to
534 secondary organic aerosols in China, *Atmospheric Chemistry and Physics*, 20, 14123-
535 14138, 2020.
- 536 Wang, K., Wang, W., Fan, C., Li, J., Lei, T., Zhang, W., Shi, B., Chen, Y., Liu, M.,
537 Lian, C., Wang, Z., and Ge, M.: Reactions of C12-C14 n-Alkylcyclohexanes with Cl
538 Atoms: Kinetics and Secondary Organic Aerosol Formation, *Environmental Science &*
539 *Technology*, 56, 4859-4870, 2022a.
- 540 Wang, S., Yuan, B., Wu, C., Wang, C., Li, T., He, X., Huangfu, Y., Qi, J., Li, X. B.,



541 Sha, Q., Zhu, M., Lou, S., Wang, H., Karl, T., Graus, M., Yuan, Z., and Shao, M.:
542 Oxygenated volatile organic compounds (VOCs) as significant but varied contributors
543 to VOC emissions from vehicles, *Atmospheric Chemistry and Physics*, 22, 9703-9720,
544 2022b.

545 Warneke, C., Geiger, F., Edwards, P. M., Dube, W., Pétron, G., Kofler, J., Zahn, A.,
546 Brown, S. S., Graus, M., Gilman, J. B., Lerner, B. M., Peischl, J., Ryerson, T. B., de
547 Gouw, J. A., and Roberts, J. M.: Volatile organic compound emissions from the oil and
548 natural gas industry in the Uintah Basin, Utah: oil and gas well pad emissions compared
549 to ambient air composition, *Atmospheric Chemistry and Physics*, 14, 10977-10988,
550 2014.

551 Wu, C., Wang, C., Wang, S., Wang, W., Yuan, B., Qi, J., Wang, B., Wang, H., Wang,
552 C., Song, W., Wang, X., Hu, W., Lou, S., Ye, C., Peng, Y., Wang, Z., Huangfu, Y., Xie,
553 Y., Zhu, M., Zheng, J., Wang, X., Jiang, B., Zhang, Z., and Shao, M.: Measurement
554 report: Important contributions of oxygenated compounds to emissions and chemistry
555 of volatile organic compounds in urban air, *Atmospheric Chemistry and Physics*, 20,
556 14769-14785, 2020.

557 Xing, L. Q., Wang, L. C., and Zhang, R.: Characteristics and health risk assessment
558 of volatile organic compounds emitted from interior materials in vehicles: a case study
559 from Nanjing, China, *Environmental Science and Pollution Research*, 25, 14789-14798,
560 2018.

561 Xu, R., Alam, M. S., Stark, C., and Harrison, R. M.: Behaviour of traffic emitted
562 semi-volatile and intermediate volatility organic compounds within the urban
563 atmosphere, *Science of The Total Environment*, 720, 2020a.

564 Xu, R., Alam, M. S., Stark, C., and Harrison, R. M.: Composition and emission
565 factors of traffic- emitted intermediate volatility and semi-volatile hydrocarbons (C₁₀–
566 C₃₆) at a street canyon and urban background sites in central London, UK, *Atmospheric
567 Environment*, 231, 2020b.

568 Yassaa, N., Meklati, B. Y., Brancaleoni, E., Frattoni, M., and Ciccioli, P.: Polar and



569 non-polar volatile organic compounds (VOCs) in urban Algiers and saharian sites of
570 Algeria, *Atmospheric Environment*, 35, 787-801, 2001.

571 Yee, L. D., Craven, J. S., Loza, C. L., Schilling, K. A., Ng, N. L., Canagaratna, M.
572 R., Ziemann, P. J., Flagan, R. C., and Seinfeld, J. H.: Effect of chemical structure on
573 secondary organic aerosol formation from C₁₂ alkanes, *Atmospheric Chemistry and*
574 *Physics*, 13, 11121-11140, 2013.

575 Yuan, B., Hu, W. W., Shao, M., Wang, M., Chen, W. T., Lu, S. H., Zeng, L. M.,
576 and Hu, M.: VOC emissions, evolutions and contributions to SOA formation at a
577 receptor site in eastern China, *Atmospheric Chemistry and Physics*, 13, 8815-8832,
578 2013.

579 Yuan, B., Koss, A. R., Warneke, C., Coggon, M., Sekimoto, K., and de Gouw, J.
580 A.: Proton-Transfer-Reaction Mass Spectrometry: Applications in Atmospheric
581 Sciences, *Chem Rev*, 117, 13187-13229, 2017.

582 Yuan, B., Warneke, C., Shao, M., and de Gouw, J. A.: Interpretation of volatile
583 organic compound measurements by proton-transfer-reaction mass spectrometry over
584 the deepwater horizon oil spill, *International Journal of Mass Spectrometry*, 358, 43-48,
585 2014.

586 Zhao, Y., Hennigan, C. J., May, A. A., Tkacik, D. S., De Gouw, J. A., Gilman, J.
587 B., Kuster, W. C., Borbon, A., and Robinson, A. L.: Intermediate-Volatility Organic
588 Compounds: A Large Source of Secondary Organic Aerosol, *Environmental Science &*
589 *Technology*, 48, 13743-13750, 2014.

590 Zhao, Y., Nguyen, N. T., Presto, A. A., Hennigan, C. J., May, A. A., and Robinson,
591 A. L.: Intermediate Volatility Organic Compound Emissions from On-Road Diesel
592 Vehicles: Chemical Composition, Emission Factors, and Estimated Secondary Organic
593 Aerosol Production, *Environmental Science & Technology*, 49, 11516-11526, 2015.

594 Zhao, Y., Nguyen, N. T., Presto, A. A., Hennigan, C. J., May, A. A., and Robinson,
595 A. L.: Intermediate Volatility Organic Compound Emissions from On-Road Gasoline
596 Vehicles and Small Off-Road Gasoline Engines, *Environmental Science & Technology*,

<https://doi.org/10.5194/egusphere-2022-880>
Preprint. Discussion started: 6 September 2022
© Author(s) 2022. CC BY 4.0 License.



597 50, 4554-4563, 2016.

598



599 **Table 1.** The formula, purity, ionization energy (IE) of the chemicals used in product
 600 ion characterization experiments are shown. The percentage of each product ion from
 601 the reactions with NO^+ ions is indicated in brackets, and the major product ions are
 602 identified in bold.

Chemicals	Formula	Purity (%)	IE ^a (eV)	Product ions (%)		
Cycloheptane	C ₇ H ₁₄	98.0%	9.82	C₇H₁₃⁺(100)		
Methylcyclohexane	C ₇ H ₁₄	99.0%	9.64	C₇H₁₃⁺(100)		
Cyclododecane	C ₁₂ H ₂₄	99.0%	9.72	C₁₂H₂₃⁺(82)	C ₈ H ₁₅ ⁺ (8)	C ₇ H ₁₃ ⁺ (10)
Hexylcyclohexane	C ₁₂ H ₂₄	98.0%	N/A ^b	C₁₂H₂₃⁺(79)	C ₈ H ₁₅ ⁺ (10)	C ₇ H ₁₃ ⁺ (11)
Bicyclohexyl	C ₁₂ H ₂₂	99.0%	9.41	C₁₂H₂₁⁺(71)	C ₅ H ₁₁ ⁺ (17)	C ₅ H ₁₃ ⁺ (<5)
				C ₇ H ₁₃ ⁺ (5)	C ₈ H ₁₅ ⁺ (<5)	C ₈ H ₁₅ ⁺ (<5)
1-Heptene	C ₇ H ₁₄	99.5%	9.34	C₇H₁₃HNO⁺(40)	C ₅ H ₉ HNO ⁺ (15)	C ₁₂ H ₂₂ ⁺ (<5)
				C ₃ H ₅ HNO ⁺ (<5)	C ₇ H ₁₄ ⁺ (<5)	C ₄ H ₇ HNO ⁺ (37)
				C₁₀H₁₉HNO⁺(51)	C ₅ H ₉ HNO ⁺ (18)	C ₆ H ₁₁ HNO ⁺ (15)
1-Decene	C ₁₀ H ₂₀	99.5%	9.42	C ₄ H ₇ HNO ⁺ (12)	C ₁₀ H ₁₉ ⁺ (<5)	C ₇ H ₁₃ HNO ⁺ (<5)
				C ₁₀ H ₂₀ ⁺ (<5)		

603 ^a NIST chemistry web book (<http://webbook.nist.gov>)

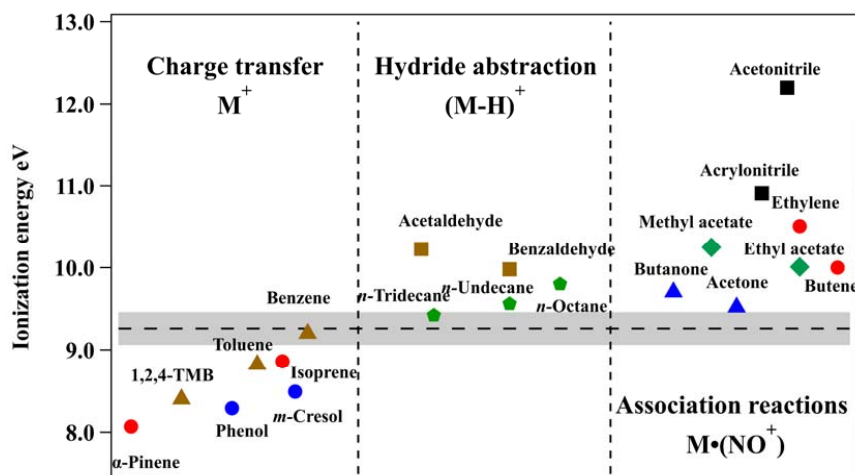
604 ^b N/A stands for “not available”



605 **Table 2.** Carbon numbers and formula, means normalized sensitivities and detection
606 limits of cycloalkanes in NO⁺ PTR-ToF-MS.

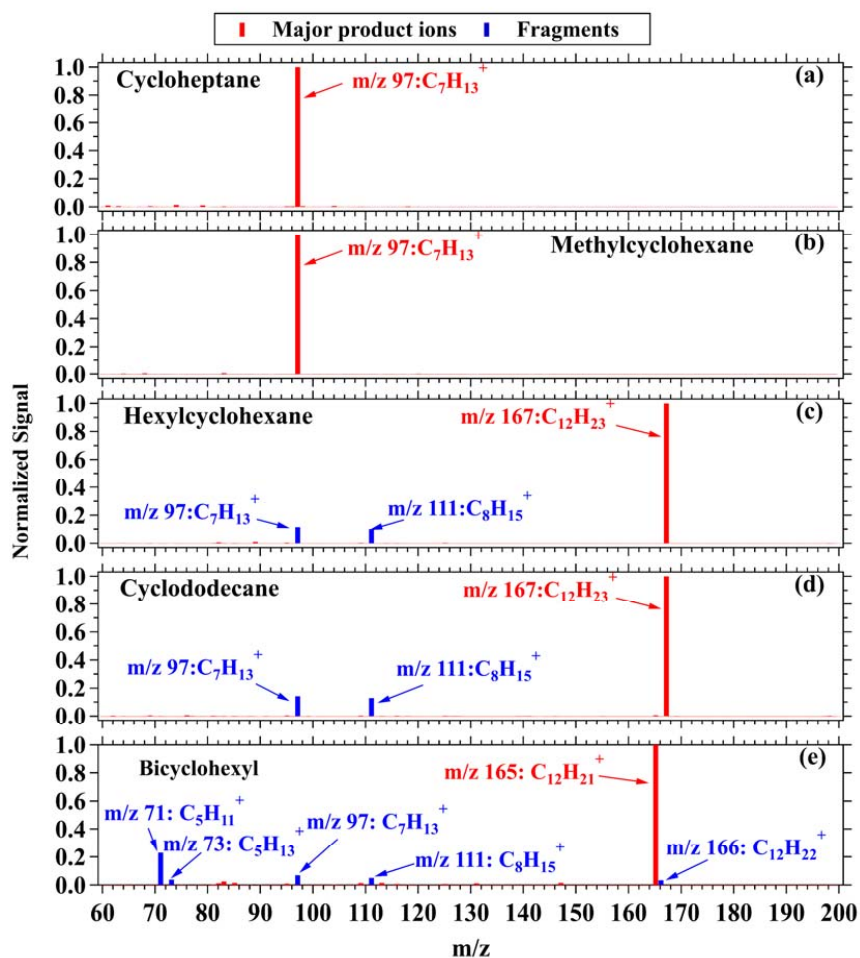
Cycloalkanes (C number)	Formula	Normalized sensitivities (ncps ppb ⁻¹)	Detection limit (ppt)	
			10s	1min
C ₁₀	C ₁₀ H ₂₀	231.3	7.20	3.04
C ₁₁	C ₁₁ H ₂₂	207.8	7.72	2.76
C ₁₂	C ₁₂ H ₂₄	223.9	7.01	2.85
C ₁₃	C ₁₃ H ₂₆	244.6	6.24	2.46
C ₁₄	C ₁₄ H ₂₈	247.9	6.22	2.40
C ₁₅	C ₁₅ H ₃₀	N/A ^a	6.67	2.54
C ₁₆	C ₁₆ H ₃₂	N/A	7.28	2.96
C ₁₇	C ₁₇ H ₃₄	N/A	7.46	3.05
C ₁₈	C ₁₈ H ₃₆	N/A	7.90	3.40
C ₁₉	C ₁₉ H ₃₈	N/A	8.21	3.61
C ₂₀	C ₂₀ H ₄₀	N/A	8.08	3.48

607 ^a N/A stands for “not available”.

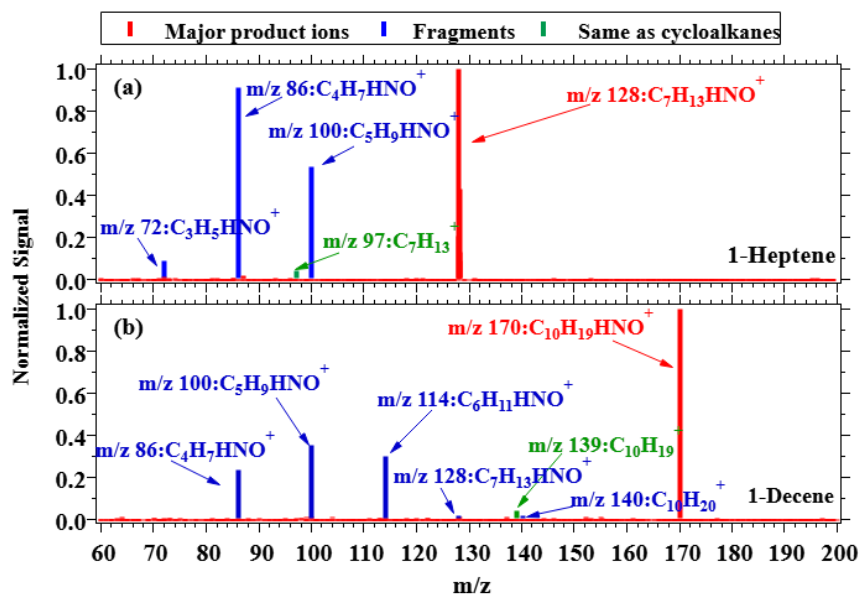


608

609 **Figure 1.** Ionization energy and reaction pathways with NO^+ ions of organic
610 compounds including alkanes (green pentagon), aromatics (brown triangle), alkenes
611 (red circle), phenolic species (blue circle), aldehydes (brown square), ketones (blue
612 triangle), esters (green diamond), and nitrogen-containing species (black square). The
613 ionization energy of NO (9.26 eV) is represented by the dashed line with shading
614 representing reported uncertainty. The IE of various organic compounds are obtained in
615 the NIST chemistry web book (<http://webbook.nist.gov>).



616
617 **Figure 2.** Mass spectra of product ions from cycloheptane (a), methylcyclohexane (b),
618 hexylcyclohexane (c), cyclododecane (d) and bicyclohexyl (e) in NO^+ PTR-ToF-MS.
619 The major product ions are shown in red, and the fragments are shown in blue.



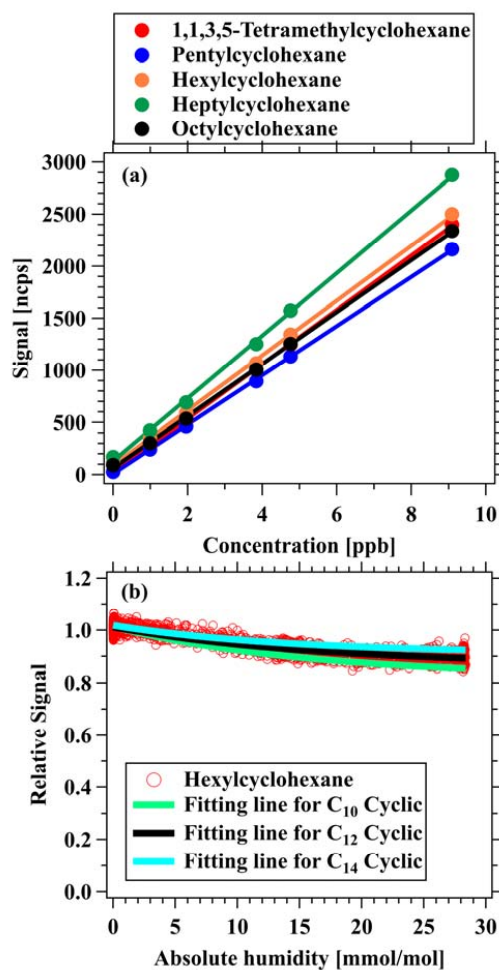
620

621 **Figure 3.** Mass spectra of product ions from 1-heptene (a), and 1-decene (b) with NO^+

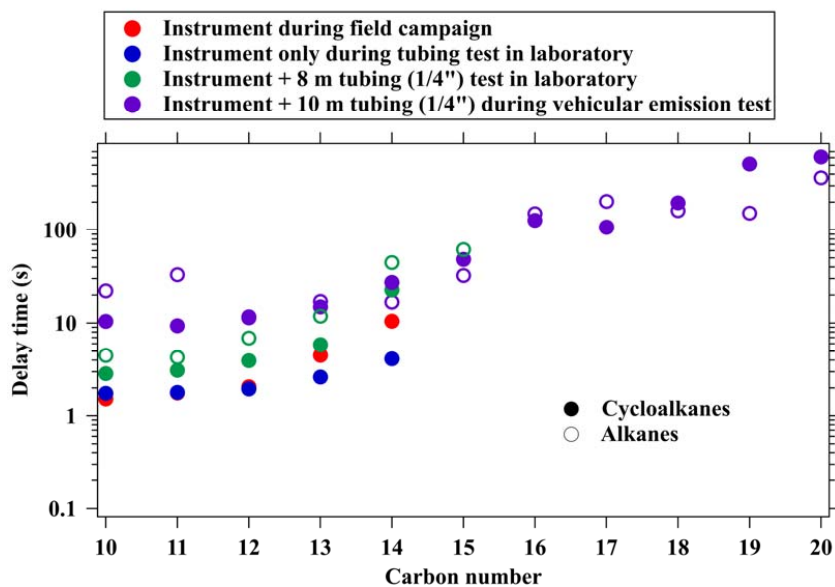
622 PTR-ToF-MS. The major product ions are shown in red. The same product ions as the

623 cycloalkanes (M-H ions) are shown in blue, and other fragments are shown in green.

624

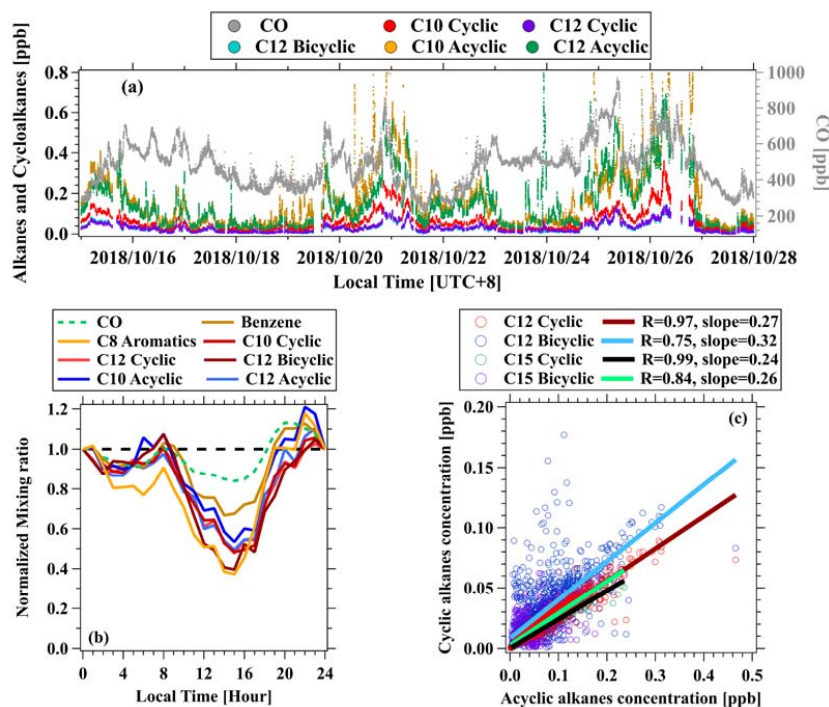


625
626 **Figure 4.** (a) Multipoint calibration curve for 1,1,3,5-tetramethylcyclohexane (red),
627 pentylcyclohexane (blue), hexylcyclohexane (orange), heptylcyclohexane (green) and
628 octylcyclohexane (black). (b) Humidity dependence of sensitivity for various
629 cycloalkanes, including measurement results for hexylcyclohexane (red markers), and
630 the fitted lines for C₁₀ cyclic alkane (green), C₁₂ cyclic alkane (black), and C₁₄ cyclic
631 alkane (blue), with the corresponding fitted functions of $y=0.82+0.19\times\exp(-0.06x)$,
632 $y=0.87+0.14\times\exp(-0.06x)$, and $y=0.90+0.11\times\exp(-0.07x)$, respectively.



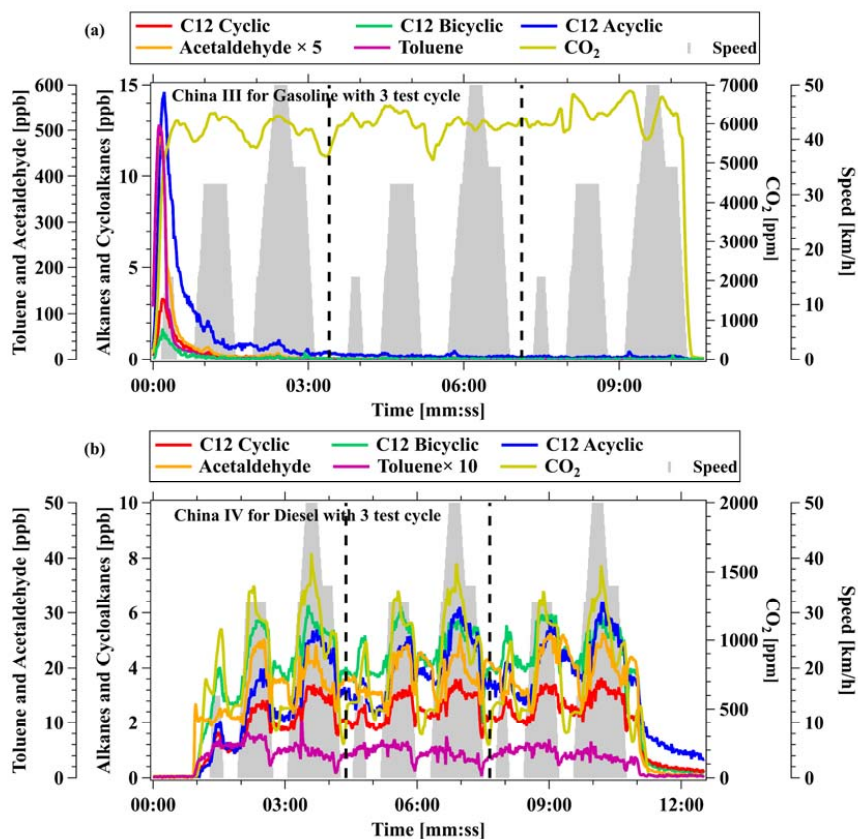
633

634 **Figure 5.** Delay time of cycloalkanes determined from measurements in the field, from
635 laboratory experiments, and vehicular emissions. The delay times of alkanes from Wang
636 et al. (2020) are also shown for comparison.



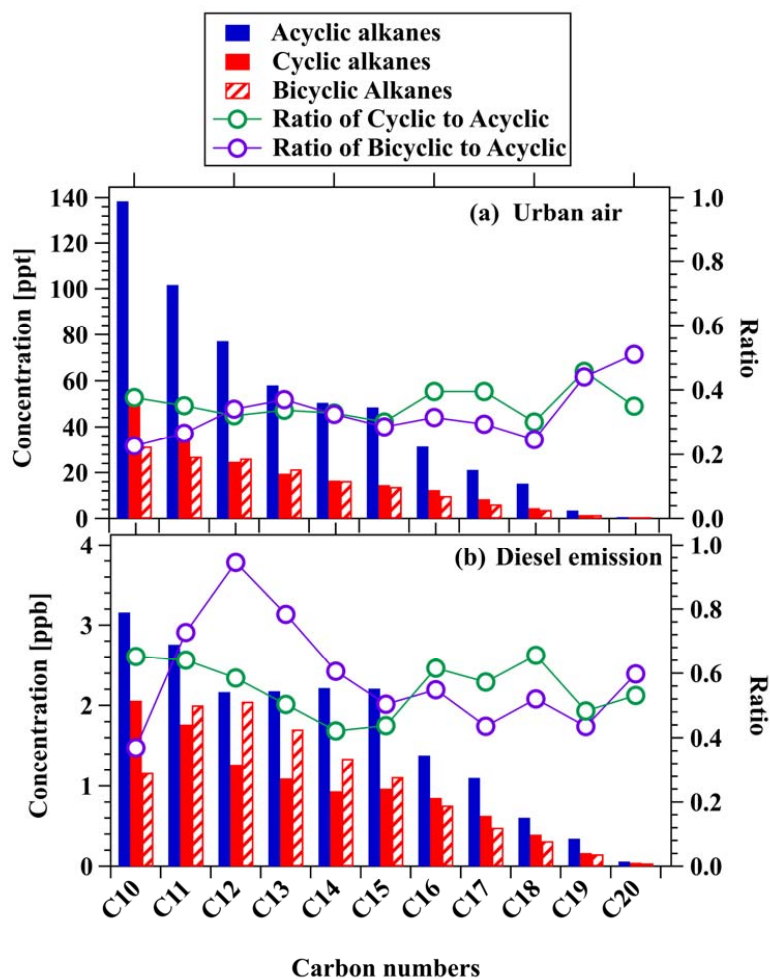
637

638 **Figure 6. (a)** Time series of CO, cyclic, bicyclic, and acyclic alkanes measured at the
639 urban site in Guangzhou. **(b)** Normalized diurnal variations of CO, benzene, C₈
640 aromatics, C₁₀ cyclic alkanes, C₁₀ acyclic alkanes, C₁₂ cyclic alkanes, C₁₂ bicyclic
641 alkanes and C₁₂ acyclic alkanes. The measurement data for each species is normalized
642 to midnight concentrations. **(c)** Scatterplots of cyclic and bicyclic alkanes to acyclic
643 alkanes with carbon atoms of 12 and 15.



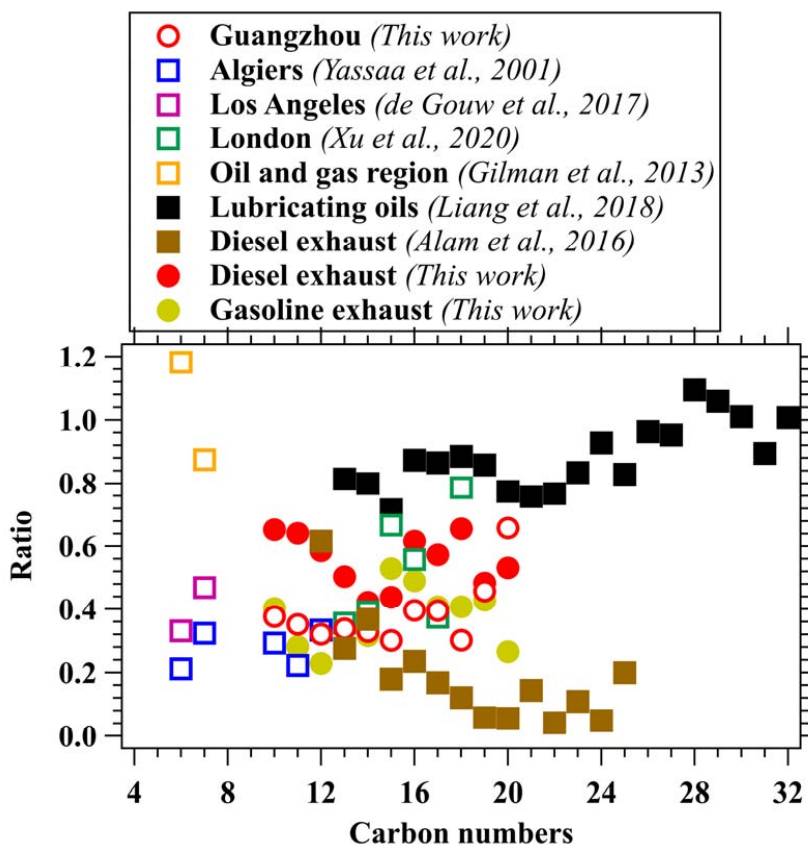
644

645 **Figure 7.** Concentrations of C₁₂ cyclic, bicyclic, and acyclic alkanes, acetaldehyde,
646 toluene, and CO₂ for **(a)** a gasoline vehicle with emission standard of China III and **(b)**
647 a diesel vehicle with emission standard of China IV. The gray shadows represent the
648 speeds of the vehicles on the chassis dynamometer.



649

650 **Figure 8.** Mean concentrations of cyclic and bicyclic alkanes and alkanes (branched +
651 linear) with different carbon numbers measured by NO^+ PTR-ToF-MS in the urban air
652 (a) and diesel emissions (b). The green and purple lines with circles represent the ratios
653 of cyclic and bicyclic alkanes to acyclic alkanes under the same carbon numbers,
654 respectively.



655

656 **Figure 9.** The concentrations ratios of cyclic alkanes to acyclic alkanes for different
657 carbon number. Measurements in various urban areas, including Guangzhou in China,
658 London in UK (Xu et al., 2020b), Los Angeles in US (de Gouw et al., 2017), Algiers in
659 Algeria (Yassaa et al., 2001), and an oil and gas region in Colorado of US (Gilman et
660 al., 2013) are also shown for comparison. Emission sources, including vehicle exhausts
661 (Alam et al., 2016) and lubricating oils (Liang et al., 2018) are also included.